REPORT

Biallelic Mutations in *UNC80* Cause Persistent Hypotonia, Encephalopathy, Growth Retardation, and Severe Intellectual Disability

Asbjørg Stray-Pedersen,[1,2,18] Jan-Maarten Cobben,[3,18] Trine E. Prescott,[4,18] Sora Lee,[5] Chunlei Cang,[5] Kimberly Aranda,[5] Sohnee Ahmed,[6] Marielle Alders,[7] Thorsten Gerstner,[8] Kathinka Aslaksen,[9] Martine Tétreault,[10] Wen Qin,[11] Taila Hartley,[11] Shalini N. Jhangiani,[1,16] Donna M. Muzny,[1,16] Maja Tarailo-Graovac,[12] Clara D.M. van Karnebeek,[13] Care4Rare Canada Consortium, Baylor-Hopkins Center for Mendelian Genomics, James R. Lupski,[1,14,15,16] Dejian Ren,[5,*] and Grace Yoon[6,17,*]

Ion channel proteins are required for both the establishment of resting membrane potentials and the generation of action potentials. Hundreds of mutations in genes encoding voltage-gated ion channels responsible for action potential generation have been found to cause severe neurological diseases. In contrast, the roles of voltage-independent "leak" channels, important for the establishment and maintenance of resting membrane potentials upon which action potentials are generated, are not well established in human disease. UNC80 is a large component of the NALCN sodium-leak channel complex that regulates the basal excitability of the nervous system. Loss-of-function mutations of *NALCN* cause infantile hypotonia with psychomotor retardation and characteristic facies (IHPRF). We report four individuals from three unrelated families who have homozygous missense or compound heterozygous truncating mutations in *UNC80* and persistent hypotonia, encephalopathy, growth failure, and severe intellectual disability. Compared to control cells, HEK293T cells transfected with an expression plasmid containing the c.5098C>T (p.Pro1700Ser) *UNC80* mutation found in one individual showed markedly decreased NALCN channel currents. Our findings demonstrate the fundamental significance of UNC80 and basal ionic conductance to human health.

Among mammalian neurons from different brain regions, there is considerable variability in basal excitability and resting membrane potentials (from approximately −85 mV to −50 mV) upon which action potentials are generated. Many mutations in voltage-gated ion channels responsible for the generation of action potentials have been found to cause severe diseases, including migraine, episodic muscle paralysis, ataxia, epilepsy, autism, and sudden cardiac death (see Jurkat-Rott et al., Kullmann and Waxman, and Catterall et al.[1–3] for reviews). In contrast, the molecular mechanisms and the role of basal excitability in human diseases are not well understood.

The resting membrane potential is primarily determined by ion channels that are open and "leaky" at rest. The basal Na^+ leak is mainly established through the NALCN Na^+-leak channel. In mouse hippocampal neurons, NALCN is responsible for ~70% of the total basal Na^+ leak.[4] NALCN is a member of the 24-transmembrane domain (24-TM) ion channel superfamily, which includes the ten voltage-gated Ca^{2+} channels and ten Na^+ channels.[5] It forms a voltage-independent, Na^+-permeable, non-selective, non-inactivating cation channel. NALCN's unique properties allow it to generate background sodium-leak currents. The balance between Na^+ influx through NALCN and K^+ efflux through other channels is predicted to generate a large dynamic range of neuronal excitability. In mammalian brains, the NALCN complex also contains UNC79 and UNC80, homologs of *C. elegans* Unc-79 and Unc-80.[6–8] In situ hybridization analysis, RNA sequencing (RNA-seq), and expression sequence-tag (EST) database searches suggest that *NALCN* (MIM: 611549), *UNC79*, and *UNC80* (MIM: 612636) are widely expressed in the brain.[4] Both UNC79 and UNC80 are large proteins (~3,000 amino acids) but do not have recognizable domains. NALCN and UNC79 do not directly interact with each other; the three components are brought together by UNC80's association with both UNC79 and NALCN.[6,7] UNC80 is required for the channel's regulation

[1]Department of Molecular and Human Genetics, Baylor College of Medicine and the Baylor-Hopkins Center for Mendelian Genomics, Houston, TX 77030, USA; [2]Norwegian National Newborn Screening Program, Oslo University Hospital, Oslo 0424, Norway; [3]Department of Pediatrics, Academic Medical Center University Hospital, Amsterdam 1105 AZ, the Netherlands; [4]Department of Medical Genetics, Oslo University Hospital, Oslo 0424, Norway; [5]Department of Biology, University of Pennsylvania, Philadelphia, PA 19104, USA; [6]Division of Clinical and Metabolic Genetics, The Hospital for Sick Children and University of Toronto, Toronto, ON M5G 1X8, Canada; [7]Department of Clinical Genetics, AMC University Hospital, Amsterdam 1105 AZ, the Netherlands; [8]Department of Pediatrics, Sørlandet Hospital, Arendal 4838, Norway; [9]Department of Pediatrics, Sørlandet Hospital, Kristiansand 4615, Norway; [10]Department of Human Genetics, McGill University and Genome Québec Innovation Center, Montréal, QC H3A 0G4, Canada; [11]The Children's Hospital of Eastern Ontario Research Institute, Ottawa, ON K1H 8L1, Canada; [12]Department of Medical Genetics, Centre for Molecular Medicine and Therapeutics, University of British Columbia, Vancouver, BC V5Z 4H4, Canada; [13]Department of Pediatrics and Centre for Molecular Medicine and Therapeutics, University of British Columbia, Vancouver, BC V5Z 4H4, Canada; [14]Department of Pediatrics, Baylor College of Medicine and Texas Children's Hospital, Houston, TX 77030, USA; [15]Department of Molecular and Human Genetics, Baylor College of Medicine, Houston, TX 77030, USA; [16]Baylor College of Medicine Human Genome Sequencing Center, Houston, TX 77030, USA; [17]Division of Neurology, The Hospital for Sick Children, University of Toronto, Toronto, ON M5G 1X8, Canada
[18]These authors contributed equally to this work
*Correspondence: dren@sas.upenn.edu (D.R.), grace.yoon@utoronto.ca (G.Y.)
http://dx.doi.org/10.1016/j.ajhg.2015.11.004.

Table 1. Clinical Characteristics of Individuals with *UNC80* Mutations

	Family 1	Family 2	Family 3	
Subject	**IV.1**	**V.5**	**II.1**	**II.3**
Age at last review	4 years	4 years	15 years	9 years
Gender	female	female	female	female
Country of parental origin	Iraq	Morocco	Norway	Norway
Parental consanguinity	+	+	−	−
Gestational age	41 weeks	41 weeks	38 weeks	40 weeks
Birth weight (percentile)	3,000 g (25^{th})	3,158 g (50^{th})	2,960 g (25^{th})	3,070 g (25^{th})
OFC at birth (percentile)	33 cm (25^{th})	unavailable	32 cm (10^{th})	35 cm (75^{th})
Hypotonia first noted	birth	birth	birth	3 months
Persistent hypotonia	+	+	+	+
Feeding difficulties	+	+	−	+
Age at G-tube insertion (degree of dependency)	2 years (dependent)	3.5 years (dependent)	15 years (supplemental use)	10 months (completely dependent)
Current age	4 years	4 years	15 years	10 years
Current height (percentile)	72 cm (<<3^{rd})	91.5 cm (<3^{rd})	144 cm (<<3^{rd})	125 cm (3^{rd})[a]
Current weight (BMI)	7.4 kg (14.3)	12.9 kg (15.4)	40.2 kg (17)	23.5 kg (15.7)[a]
Current OFC (percentile)	43 cm (<<3^{rd}, or −4 SD)	47 cm (2^{nd}, or −1 SD)	51.5 cm (3^{rd})	50.5 cm (10^{th})[a]
Ophthalmology	punctate keratopathy, normal visual evoked potentials	alternating esotropia, normal visual evoked potentials	esotropia, normal vision	esotropia, normal vision, normal visual evoked potentials
Hypotonic facies	+	+	+	+
Small hands and feet	+	−	+	+
Severe global developmental delay and intellectual disability	+	+	+	+
Communication	no speech	no speech	no speech, babbles socially, expressive body language	no speech, babbles socially, expressive body language
Psychosocial	poor eye contact, minimal interest in surroundings	sociable, studies faces with interest	sociable, content, interested in surroundings	sociable, content, interested in surroundings
Gross motor	unable to sit, non-ambulatory	sits without support, non-ambulatory	sits with support, pulls to stand, walks with a walker	sits without support, stands and walks with support
Fine motor	transfers objects across midline	brings food to mouth, manipulates toys	brings food to mouth, manipulates toys	Manipulates objects
Muscle weakness	+, MRC grade 3/5	difficult to assess due to severe hypotonia	+, MRC grade 4/5	+, MRC grade 4/5
Seizures, age of onset	+, 3 months (none since 3 years old)	+, 3 years and 10 months	+, 6 months	+, 3 years
Seizure types	generalized tonic-clonic	generalized tonic-clonic	myoclonic, atonic, generalized tonic-clonic, atypical absences	atonic, atypical absences
Current anti-convulsive therapy	clonazepam	valproate, rivotril	valproate, lamotrigine, levetiracetam, vagal nerve stimulator	valproate
Severe constipation	+	+	+	+
Tactile aversion	−	−	+	+

(*Continued on next page*)

Table 1. ***Continued***

	Family 1	Family 2	Family 3	
Subject	**IV.1**	**V.5**	**II.1**	**II.3**
Hypersensitivity for stimuli	−	+	+	+
Sleep disturbance	+, obstructive sleep apnea	+	−	−
Brain MRI	thin corpus callosum	no structural anomalies	no structural anomalies	no structural anomalies
EEG	encephalopathic background with occasional spike and wave discharges	encephalopathic background pattern with frequent multifocal discharges	encephalopathic background activity with frequent spike and wave discharges	encephalopathic background activity with frequent spike and wave discharges
Other	non-specific myopathic changes on muscle biopsy	not reported	mild scoliosis, euthyroid	milk protein intolerance in infancy, euthyroid
Mutation[b]	chr2:210783340C>T	chr2:210824431G>C	chr2:210832310T>A	chr2:210685105delA
UNC80 (GenBank: NM_032504.1)	c.5098C>T	c.7607G>C	c.7757T>A	c.2033delA
Exon number	32	50	51	13
Predicted effect on protein	p.Pro1700Ser	p.Arg2536Thr, predicted to cause aberrant splicing	p. Leu2586*	p.Asn678Thrfs*15
Type of mutation	missense	missense	stop	frameshift insertion

Abbreviations are as follows: +, present; −, not present; OFC, occipital frontal circumference; MRC, Medical Research Council scale for muscle strength.
[a]Measurements for individual II.3 were taken at the last examination at the age of 9 years, rather than at the current age.
[b]Based on UCSC Genome Browser GRCh37.

by extracellular Ca^{2+} through a G-protein-dependent pathway and by neuropeptides, such as substance P, through a G-protein-independent pathway that also requires the Src family of kinases.[5]

In worms and flies, mutations in *Nalcn*, *Unc-79*, and *Unc-80* lead to uncoordinated movements, abnormal circadian rhythms, and altered sensitivity to anesthetics.[9–13] In mice, knocking out *Nalcn* or *Unc79* leads to severe apnea and neonatal lethality.[4,5,7] In humans, inherited homozygous loss-of-function *NALCN* mutations cause infantile hypotonia with psychomotor retardation and characteristic facies (IHPRF [MIM: 615419]).[14,15] De novo heterozygous *NALCN* mutations are also found in individuals with arthrogryposis, hypotonia, intellectual disability, and developmental delay.[16,17]

Despite its widespread expression in the brain, the in vivo function of *UNC80* is largely unknown, and no mutations in mammals have been reported. We report the identification and characterization of *UNC80* mutations as the cause of severe neurological phenotypes in four female individuals from three unrelated families.

The four subjects have similar phenotypes characterized by severe hypotonia of neonatal onset and that persists until adolescence, motor delays, lack of independent ambulation, constipation, encephalopathy, seizures, absent speech, and severe intellectual disability. The clinical features and genetic results of all subjects are summarized in Table 1 and Figure 1. Research protocols were approved in each country via institutional research boards and regional ethics committees, in keeping with national guidelines and the principles laid out in the Declaration of Helsinki. For the Norwegian family (F3), molecular analyses were performed in accordance with the Norwegian National Biotechnology Act. All parents provided written informed consent for study participation for themselves and their children, as well as for publication of clinical information, molecular findings, and photographs.

For family 1, the whole-exome sequencing (WES) library preparation, exon capture, and sequencing were performed at the Genome Québec Innovation Center (Montréal) as previously described.[18] Genomic DNA was captured with the SureSelect Human 50 Mb All Exon V5 kit (Agilent Technologies). Sequencing was performed on an Illumina HiSeq 2000 (Illumina) with paired-end 100-bp reads. A mean coverage of 134× was obtained, and 97% of the bases were covered at more than 10×. WES trio average coverage was 55×. Read alignment, variant calling, and annotation were done with a pipeline based on the Burrows-Wheeler Aligner (BWA), SAMtools, ANNOVAR, and custom annotation scripts, and reads were aligned to the reference human genome (UCSC Genome Browser hg19).

For family 2, DNA capture was performed with the SeqCap EZ Exome v.3.0 (Roche Nimblegen). Sequencing was performed on an Illumina HiSeq 2000 (Illumina) with paired-end 100-bp reads. A mean coverage of 76× was obtained, and 94% of the bases were covered at more than 10×. Read alignment to the reference human genome (hg19) and variant calling were done with a pipeline based on BWA-MEM v.0.7 and the Genome Analysis Toolkit (GATK v.3.1-1-g07a4bf8). Variant annotation and prioritizing were done with Cartagenia NGS Bench (Cartagenia).

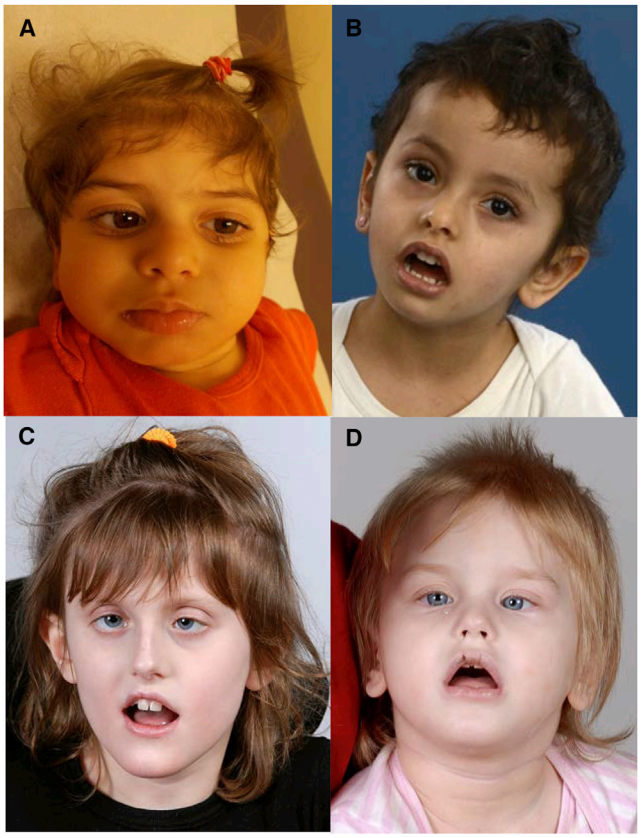

Figure 1. Clinical Photographs of All Four Subjects
(A) Subject F1-IV.1 at the age of 4 years.
(B) Subject F2-V.5 at the age of 3 years.
(C) Subject F3-II.1 at the age of 9 years.
(D) Subject F3-II.3 at the age of 3 years.

Four individuals from family 3 were tested and included in the Center for Mendelian Genomics project at the Baylor College of Medicine (BCM) in Houston, Texas. The WES method used at the BCM-HGSC (Human Genome Sequencing Center) has previously been described.[19] In brief, DNA was prepared for Illumina paired-end libraries, and capture was performed with the in-house-developed BCM-HGSC Core design and sequenced on the Illumina HiSeq 2500 platform (Illumina). Data produced was processed through the HGSC-developed Mercury pipeline, available in the cloud,[20] to produce variant call format files (.vcf) with the Atlas2 variant calling method.[21–23] Variants were annotated with the in-house-developed "Cassandra"[24] annotation pipeline, based on ANNOVAR.[25] Variants of interest were selected on the basis of inheritance pattern, rarity, and evaluation of possible genotype-phenotype correlation by knowledge of gene function, pathway, expression pattern, and results from other model organisms. Alamut v.2.4.6 (Interactive Biosoftware) was used in evaluation of pathological relevance. Additional support was sought by application of computational prediction tools (PhyloP, SIFT, PolyPhen-2, LRT, and MutationTaster). All *UNC80* variants were confirmed by Sanger sequencing. Unaffected family members were also Sanger sequenced to confirm that the variant segregated with disease. Sanger sequencing was performed on genomic DNA from peripheral blood. Primers for Sanger sequencing were designed with Primer3 software and sequenced on an ABI 3730 sequencer (Applied Biosystems, Life Technologies), and sequence data was analyzed with SeqScape v.2.7 (Life Technologies) and 4Peaks.

Subject F1-IV.1 was found to be homozygous for a c.5098C>T missense variant (p.Pro1700Ser) in exon 32 of *UNC80* (GenBank: NM_032504.1). The variant is predicted to be deleterious and is present at a position completely conserved among all animals (Figure S3). The subject's father was unable to be tested, but her mother was confirmed to be a carrier of the variant (Figure 2).

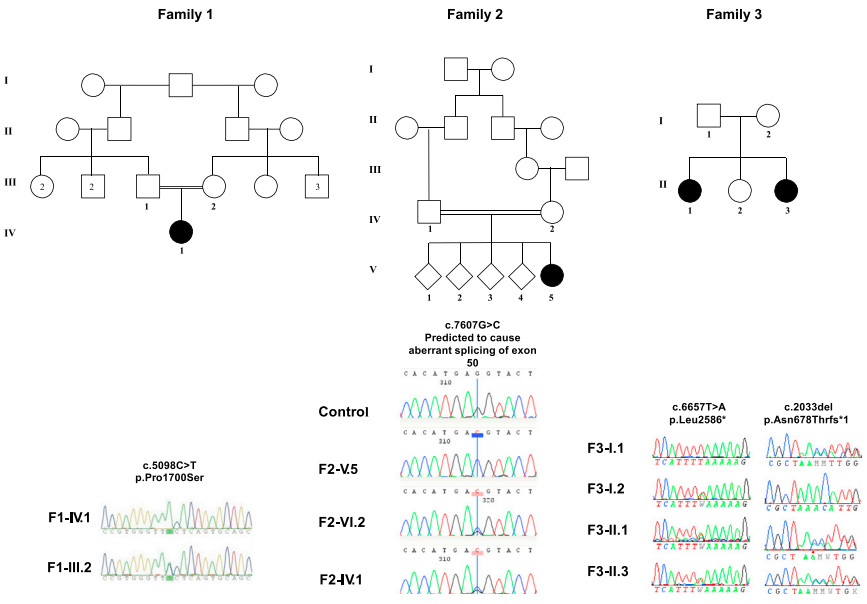

Figure 2. Pedigrees and Chromatograms from All Three Families
Affected individuals are shaded in black.

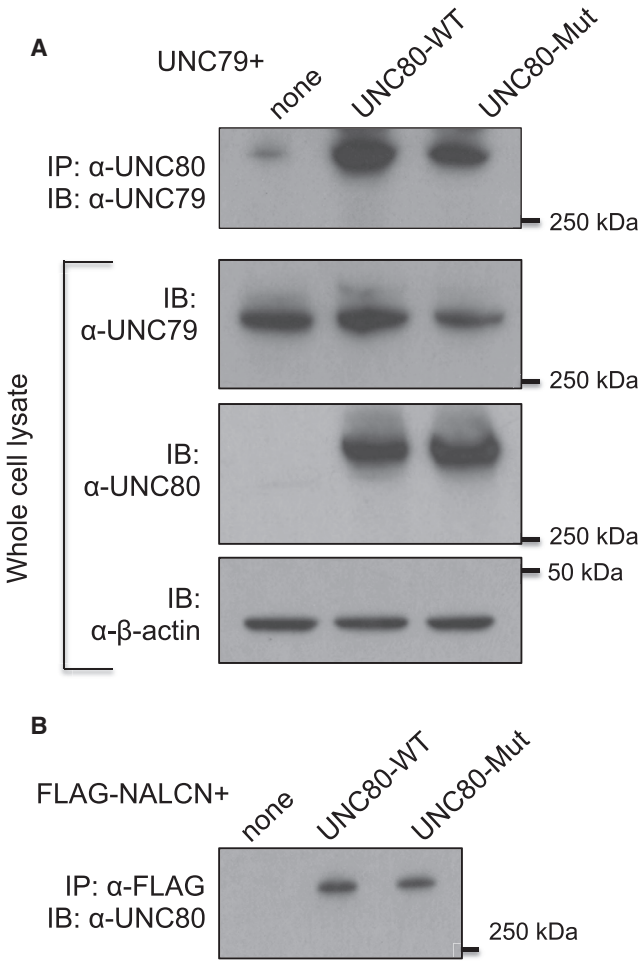

Figure 3. Variant UNC80 Associates with UNC79 and NALCN
(A) Cells were transfected with *UNC79* alone or together with WT or variant *Unc80* as indicated in each lane. Immunoprecipitates (IP) with an anti-UNC80 antibody were blotted (IB) with anti-UNC79 to allow us to probe the association between UNC79 and UNC80 (upper panel). Total cell lysates (lower three panels) were blotted with anti-UNC79 or anti-UNC80 antibodies for comparison of protein amounts. Immunoblotting with anti-β-actin (lower panel) was used as a control for sample loading.
(B) Cells were transfected with FLAG-tagged *NALCN* alone or together with the WT or variant *Unc80*, as indicated. Immunoprecipitates with anti-FLAG were blotted with anti-UNC80 to allow us to probe the association between UNC80 and NALCN. For immunoprecipitation, cells were solubilized in lysis buffer (50 mM Tris-HCl, 150 mM NaCl, 1% NP-40, 1× PIC [Roche]) and immunoprecipitated with anti-UNC80 (2 μg/ml)[7] or anti-FLAG (5 μg/ml, no. F3165 [Sigma]). The immune complexes were analyzed by western blot with anti-UNC80 (2.2 μg/ml) or anti-UNC79 (3 μg/ml). Cell lysates (inputs) were also analyzed by western blot with anti-UNC80 or anti-β-actin (1:1,000, no. 4970S [Cell Signaling]) as indicated.

Subject F2-V.5 had a homozygous missense variant in *UNC80*, c.7607G>C (p.Arg2536Thr). G7607 is the last nucleotide of exon 50. The c.7607G>C variant disrupts the "AG" exonic sequence commonly found in exon-intron junctions upstream of the conserved splice-donor sequence "GT." The variant is predicted by five independent methods to affect splicing efficiency (Figure S4). Splicing studies of *UNC80* were not performed because *UNC80* is not expressed in peripheral leukocytes and no other tissue was available from this individual. The variant (p.Arg2536Thr) is also predicted to neutralize a charged residue highly conserved in all animals (Figure S5), suggesting that the variant disrupts protein function even in transcripts that are correctly spliced. Splicing analysis in neurons and functional characterization of the corresponding protein are required to determine the molecular consequence of this variant. Both healthy parents of subject F2-V.5 were heterozygous carriers, and all four healthy siblings were either heterozygous or bi-allelic wild-type (WT) at this nucleotide position (Figure 2). Subject F3-II.1 and subject F3-II.3 were both found to be compound heterozygous for the following *UNC80* variants: c.2033delA (p.Asn678Thrfs*15) and c.7757T>A (p.Leu2586*) (GenBank: NM_032504.1). Both parents were found to be heterozygous carriers of one of the variants (Figure 2). None of the variants were present in publically available databases (dbSNP, 1000 Genomes, and the ExAC Browser), and the c.5098C>T variant was found in the heterozygous state in one individual in the database of over 3,000 exomes at the Center for Mendelian Genomics.

The three mutations in subjects F2-V.5, F3-II.1, and F3-II.3 are predicted to lead to disruption (in F2-V.5, due to aberrant splicing) or truncation (in F3-II.1 and F3-II.3) of UNC80 and are most likely loss-of-function mutations. To determine whether the c.5098C>T missense variant (p.Pro1700Ser) in subject F1-IV.1 affects expression and function of UNC80, we introduced the variant into mouse *Unc80* cDNA, which encodes a protein with 97% identity to the human UNC80 and has been functionally characterized. The mouse *Unc80* cDNA (GenBank: FJ210934) was cloned into the EcoRI and NotI sites of vector pcDNA3.1. The p.Pro1769Ser variant (equivalent to human p.Pro1700Ser) was introduced with the Gibson assembly method. The sequences of the primers used for mutagenesis are as follows: 5′-GTTCGACCCTCCGTGGGTCtCT CAGTGCAGCGGGAGTG-3′ (forward), 5′-CACTCCCGCT GCACTGAGAGACCCACGGAGGGTCGAAC-3′ (reverse). The mutation was confirmed with Sanger sequencing.

We transfected the WT and variant *Unc80* into human HEK293T cells (from ATCC, maintained in DMEM [GIBCO] supplemented with 10% FBS [Atlanta Biologicals] and 1× Glutamax [GIBCO]; transfection done with Lipofectamine 2000 as the transfection reagent). The *Unc80* variant yielded an amount of protein comparable to that yielded by the WT *Unc80* (Figure 3A, lower two panels), suggesting that this missense variant does not disrupt production of the protein. The variant protein also retained its ability to associate with UNC79 (Figure 3A) and NALCN (Figure 3B), which was tested by co-immunoprecipitation.

We next used electrophysiological assays to test whether the p.Pro1769Ser (mouse equivalent of p.Pro1700Ser) variant affects the function of UNC80. A unique property of UNC80 is its ability to scaffold Src kinase and to enhance

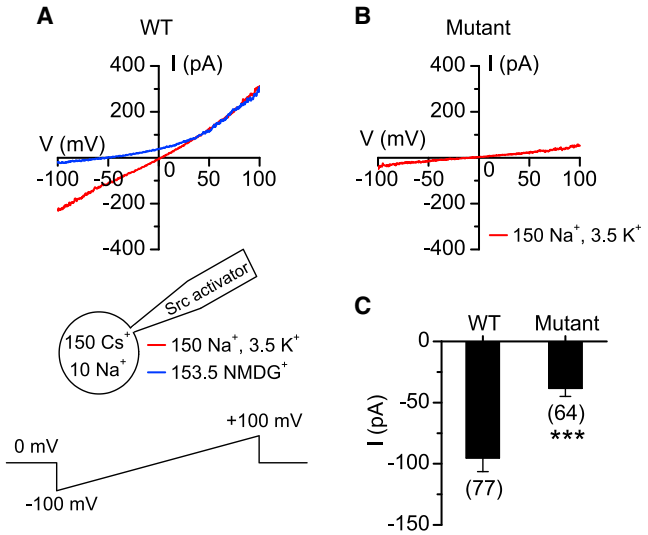

Figure 4. Altered Function in Variant UNC80

(A and B) Representative NALCN currents recorded in HEK293T cells co-transfected with *NALCN* and WT *Unc80* (A) or the mutant version of *Unc80* (B). Whole-cell currents were recorded with a voltage ramp from −100 mV to +100 mV in 1 s (Vh = 0 mV, illustrated in the lower panel of A). In cells with currents larger than 50 pA, NMDG was used to substitute Na^+ and K^+ to confirm that the cells had no non-specific leak, as demonstrated by the abolishment of inward currents with ion substitution.

(C) Summary of the current amplitudes recorded at −100 mV. Numbers of cells recorded are in parentheses. Data were presented as mean ± SEM. *$p < 0.05$. ***$p < 0.001$. For patch clamp recordings, cells in a 35-mm dish (~90% confluency) were transfected with 3 μg plasmids DNA with Lipofectamine 2000 for ~40 hr and plated onto polylysine-coated coverslips. Recordings were done 40–48 hr after transfection. Cells with GFP fluorescence intensity within the top 20%–30% on each coverslip were selected for patch clamp recordings. Signal was acquired with an amplifier (Axopatch 200B or Multiclamp 700B) and a Digidata 1440A data acquisition system controlled by PClamp software (Molecular Device). The pipette solution contained 150 mM Cs, 120 mM Mes, 10 mM NaCl, 10 mM EGTA, 4 mM $CaCl_2$, 0.3 mM Na2GTP, 2 mM Mg-ATP, 10 mM HEPES and 2 μM Src family kinase activator (pH 7.4; from Santa Cruz). Bath solutions contained 150 mM NaCl, 3.5 mM KCl, 1 mM MgCl2, 1.2 mM CaCl2, 20 mM glucose, and 10 mM HEPES (pH 7.4). In the NMDG bath, Na^+ and K^+ were replaced by $NMDG^+$. Liquid junction potentials were corrected online.

NALCN currents through a Src-dependent pathway.[6,8] We recorded NALCN currents from HEK293T cells that we co-transfected with *NALCN* cDNA (human isoform,[7] in a pTracer vector expressing GFP under a separate promoter) and WT or variant *Unc80* by using patch clamp pipettes containing a peptide Src activator (Figure 4A, lower panel). Compared to those in cells transfected with WT *Unc80*, the sizes of the currents were significantly reduced in cells expressing the variant (Figures 4B and 4C).

In summary, our studies reveal a genetic cause for global developmental delay and neurological dysfunction and demonstrate the importance of *UNC80* in humans. From a motor perspective, all four individuals were significantly delayed in sitting; one individual was still unable to achieve this at the age of 4 years. None of the individuals were able to ambulate independently. These symptoms are comparable with those observed in individuals with loss-of-function *NALCN* mutations.[14,15] Unlike individuals with *NALCN* mutations, our four *UNC80* individuals show no true facial dysmorphism, although their faces are characterized by features related to severe hypotonia. All individuals in our study were described as encephalopathic, both clinically and on electroencephalogram (EEG) monitoring. Growth failure, severe constipation, and the feeding difficulties requiring G-tube insertion might be due, in part, to dysfunctional muscle coordination via neuronal compromise; however, standardized evaluation of swallowing function for all individuals would be required to confirm this. Subject F1-IV.1 also had severe sleep disturbance, including complete reversal of her sleep-wake cycle, which was resistant to treatment with melatonin. Subject F2-V.5 also had sleep disturbance, including difficulty falling asleep. In flies and mice, NALCN is essential for the depolarization of clock neurons in the morning and the maintenance of normal circadian rhythms.[26] It is possible that abnormal UNC80 prevents activation of the NALCN complex and inhibits the ability of pacemaker neurons to maintain basal sleep-wake rhythm.

Compared to phenotypes associated with mutations found in known neuronal genes, the neurological phenotypes we describe in these four *UNC80* individuals are at the severe end of the spectrum. This underscores the pivotal importance of leak ion channel genes and the associated basal excitability in human health and disease.

Supplemental Data

Supplemental Data include additional case histories, five figures, and one table and can be found with this article online at http://dx.doi.org/10.1016/j.ajhg.2015.11.004.

Acknowledgments

We would like to thank the participants and families for their contribution to this study. This work was selected for study by the Care4Rare Canada (Enhanced Care for Rare Genetic Diseases in Canada) Consortium Gene Discovery Steering Committee: Kym Boycott (lead; University of Ottawa), Alex MacKenzie (co-lead; University of Ottawa), J.M. (McGill University), Michael Brudno (University of Toronto), Dennis Bulman (University of Ottawa), and David Dyment (University of Ottawa). We also thank Hanne S. Sorte and Mari Ann Kulseth (Department of Medical Genetics, Oslo University Hospital) for excellent technical assistance. J.R.L. has stock ownership in 23andMe, is a paid consultant for Regeneron Pharmaceuticals, has stock options in Lasergen, is a member of the Scientific Advisory Board of Baylor Miraca Genetics Laboratories, and is a co-inventor on multiple US and European patents related to molecular diagnostics for inherited neuropathies, eye diseases, and bacterial genomic fingerprinting. The Department of Molecular and Human Genetics at Baylor College of Medicine (J.R.L.) derives revenue from the chromosomal microarray analysis and clinical exome sequencing offered in the Baylor Miraca Genetics Laboratory (http://www.bmgl.com). This work was supported, in part, by funding from the NIH to

D.R. (NS055293 and NS074257). Funding was also received from Genome Canada, the Canadian Institutes of Health Research, the Ontario Genomics Institute, Ontario Research Fund, Genome Quebec, Children's Hospital of Eastern Ontario Foundation, and The Hospital for Sick Children. The Baylor-Hopkins Center for Mendelian Genomics is supported by the National Human Genome Research Institute and the National Heart Lung and Blood Institute (U54HG006542).

Received: September 15, 2015
Accepted: November 4, 2015
Published: December 17, 2015

Web Resources

The URLs for data presented herein are as follows:

1000 Genomes, http://browser.1000genomes.org
4Peaks, http://nucleobytes.com/4peaks
dbSNP, http://www.ncbi.nlm.nih.gov/projects/SNP/
ExAC Browser, http://exac.broadinstitute.org/
GenBank, http://www.ncbi.nlm.nih.gov/genbank/
GeneMatcher, https://genematcher.org/
MutationTaster, http://www.mutationtaster.org/
NHLBI Exome Sequencing Project (ESP) Exome Variant Server, http://evs.gs.washington.edu/EVS/
OMIM, http://www.omim.org/
PolyPhen-2, http://genetics.bwh.harvard.edu/pph2/
SIFT, http://sift.bii.a-star.edu.sg/
UCSC Genome Browser, http://genome.ucsc.edu

References

1. Jurkat-Rott, K., Lerche, H., Weber, Y., and Lehmann-Horn, F. (2010). Hereditary channelopathies in neurology. Adv. Exp. Med. Biol. *686*, 305–334.
2. Kullmann, D.M., and Waxman, S.G. (2010). Neurological channelopathies: new insights into disease mechanisms and ion channel function. J. Physiol. *588*, 1823–1827.
3. Catterall, W.A., Dib-Hajj, S., Meisler, M.H., and Pietrobon, D. (2008). Inherited neuronal ion channelopathies: new windows on complex neurological diseases. J. Neurosci. *28*, 11768–11777.
4. Lu, B., Su, Y., Das, S., Liu, J., Xia, J., and Ren, D. (2007). The neuronal channel NALCN contributes resting sodium permeability and is required for normal respiratory rhythm. Cell *129*, 371–383.
5. Ren, D. (2011). Sodium leak channels in neuronal excitability and rhythmic behaviors. Neuron *72*, 899–911.
6. Lu, B., Su, Y., Das, S., Wang, H., Wang, Y., Liu, J., and Ren, D. (2009). Peptide neurotransmitters activate a cation channel complex of NALCN and UNC-80. Nature *457*, 741–744.
7. Lu, B., Zhang, Q., Wang, H., Wang, Y., Nakayama, M., and Ren, D. (2010). Extracellular calcium controls background current and neuronal excitability via an UNC79-UNC80-NALCN cation channel complex. Neuron *68*, 488–499.
8. Wang, H., and Ren, D. (2009). UNC80 functions as a scaffold for Src kinases in NALCN channel function. Channels (Austin) *3*, 161–163.
9. Humphrey, J.A., Hamming, K.S., Thacker, C.M., Scott, R.L., Sedensky, M.M., Snutch, T.P., Morgan, P.G., and Nash, H.A. (2007). A putative cation channel and its novel regulator: cross-species conservation of effects on general anesthesia. Curr. Biol. *17*, 624–629.
10. Jospin, M., Watanabe, S., Joshi, D., Young, S., Hamming, K., Thacker, C., Snutch, T.P., Jorgensen, E.M., and Schuske, K. (2007). UNC-80 and the NCA ion channels contribute to endocytosis defects in synaptojanin mutants. Curr. Biol. *17*, 1595–1600.
11. Pierce-Shimomura, J.T., Chen, B.L., Mun, J.J., Ho, R., Sarkis, R., and McIntire, S.L. (2008). Genetic analysis of crawling and swimming locomotory patterns in C. elegans. Proc. Natl. Acad. Sci. USA *105*, 20982–20987.
12. Yeh, E., Ng, S., Zhang, M., Bouhours, M., Wang, Y., Wang, M., Hung, W., Aoyagi, K., Melnik-Martinez, K., Li, M., et al. (2008). A putative cation channel, NCA-1, and a novel protein, UNC-80, transmit neuronal activity in C. elegans. PLoS Biol. *6*, e55.
13. Nash, H.A., Scott, R.L., Lear, B.C., and Allada, R. (2002). An unusual cation channel mediates photic control of locomotion in Drosophila. Curr. Biol. *12*, 2152–2158.
14. Köroğlu, Ç., Seven, M., and Tolun, A. (2013). Recessive truncating NALCN mutation in infantile neuroaxonal dystrophy with facial dysmorphism. J. Med. Genet. *50*, 515–520.
15. Al-Sayed, M.D., Al-Zaidan, H., Albakheet, A., Hakami, H., Kenana, R., Al-Yafee, Y., Al-Dosary, M., Qari, A., Al-Sheddi, T., Al-Muheiza, M., et al. (2013). Mutations in NALCN cause an autosomal-recessive syndrome with severe hypotonia, speech impairment, and cognitive delay. Am. J. Hum. Genet. *93*, 721–726.
16. Chong, J.X., McMillin, M.J., Shively, K.M., Beck, A.E., Marvin, C.T., Armenteros, J.R., Buckingham, K.J., Nkinsi, N.T., Boyle, E.A., Berry, M.N., et al.; University of Washington Center for Mendelian Genomics (2015). De novo mutations in NALCN cause a syndrome characterized by congenital contractures of the limbs and face, hypotonia, and developmental delay. Am. J. Hum. Genet. *96*, 462–473.
17. Aoyagi, K., Rossignol, E., Hamdan, F.F., Mulcahy, B., Xie, L., Nagamatsu, S., Rouleau, G.A., Zhen, M., and Michaud, J.L. (2015). A Gain-of-Function Mutation in NALCN in a Child with Intellectual Disability, Ataxia, and Arthrogryposis. Hum. Mutat. *36*, 753–757.
18. Tetreault, M., Fahiminiya, S., Antonicka, H., Mitchell, G.A., Geraghty, M.T., Lines, M., Boycott, K.M., Shoubridge, E.A., Mitchell, J.J., Michaud, J.L., and Majewski, J.; Care4Rare Canada Consortium (2015). Whole-exome sequencing identifies novel ECHS1 mutations in Leigh syndrome. Hum. Genet. *134*, 981–991.
19. Yang, Y., Muzny, D.M., Reid, J.G., Bainbridge, M.N., Willis, A., Ward, P.A., Braxton, A., Beuten, J., Xia, F., Niu, Z., et al. (2013). Clinical whole-exome sequencing for the diagnosis of mendelian disorders. N. Engl. J. Med. *369*, 1502–1511.
20. Reid, J.G., Carroll, A., Veeraraghavan, N., Dahdouli, M., Sundquist, A., English, A., Bainbridge, M., White, S., Salerno, W., Buhay, C., et al. (2014). Launching genomics into the cloud: deployment of Mercury, a next generation sequence analysis pipeline. BMC Bioinformatics *15*, 30.
21. Challis, D., Yu, J., Evani, U.S., Jackson, A.R., Paithankar, S., Coarfa, C., Milosavljevic, A., Gibbs, R.A., and Yu, F. (2012). An integrative variant analysis suite for whole exome next-generation sequencing data. BMC Bioinformatics *13*, 8.
22. Danecek, P., Auton, A., Abecasis, G., Albers, C.A., Banks, E., DePristo, M.A., Handsaker, R.E., Lunter, G., Marth, G.T., Sherry, S.T., et al.; 1000 Genomes Project Analysis Group (2011). The variant call format and VCFtools. Bioinformatics *27*, 2156–2158.

23. Li, H., and Durbin, R. (2009). Fast and accurate short read alignment with Burrows-Wheeler transform. Bioinformatics *25*, 1754–1760.
24. Bainbridge, M.N., Wiszniewski, W., Murdock, D.R., Friedman, J., Gonzaga-Jauregui, C., Newsham, I., Reid, J.G., Fink, J.K., Morgan, M.B., Gingras, M.C., et al. (2011). Whole-genome sequencing for optimized patient management. Sci. Transl. Med. *3*, 87re3.
25. Wang, K., Li, M., and Hakonarson, H. (2010). ANNOVAR: functional annotation of genetic variants from high-throughput sequencing data. Nucleic Acids Res. *38*, e164.
26. Flourakis, M., Kula-Eversole, E., Hutchison, A.L., Han, T.H., Aranda, K., Moose, D.L., White, K.P., Dinner, A.R., Lear, B.C., Ren, D., et al. (2015). A Conserved Bicycle Model for Circadian Clock Control of Membrane Excitability. Cell *162*, 836–848.

The American Journal of Human Genetics

Supplemental Data

Biallelic Mutations in *UNC80* Cause Persistent Hypotonia, Encephalopathy, Growth Retardation, and Severe Intellectual Disability

Asbjørg Stray-Pedersen, Jan-Maarten Cobben, Trine E. Prescott, Sora Lee, Chunlei Cang, Kimberly Aranda, Sohnee Ahmed, Marielle Alders , Thorsten Gerstner, Kathinka Aslaksen, Martine Tétreault, Wen Qin, Taila Hartley, Shalini N. Jhangiani, Donna M. Muzny, Maja Tarailo-Graovac, Clara D.M. van Karnebeek, Care4Rare Canada Consortium, Baylor-Hopkins Center for Mendelian Genomics, James R. Lupski, Dejian Ren, and Grace Yoon

Supplemental Data

Supplemental Case Histories and Figures

Subject F1-IV.1

This is a four-year-old girl who is the only child of healthy Iraqi parents who are first cousins. Family history is otherwise non-contributory. She was born via spontaneous vaginal delivery at 41 weeks gestation after a normal pregnancy, with a birth weight of 3000 g and Apgar scores of 9 at one and five minutes**.** She was hypotonic, with feeding difficulties and severe constipation. At age 2 weeks, she was investigated for possible Hirschsprung's disease; however, a rectal biopsy was normal. At age three months she developed generalized tonic-clonic seizures. These were well-controlled with Clonazepam, and she has been seizure-free for the past year. A subglottic web was detected in conjunction with investigations for frequent recurrent febrile episodes between ages four and nine months. At age 2 years a G-tube was placed due to severe feeding difficulties, however she continues to fail to thrive. Currently at age four years, she is able to sit independently for a few seconds. She rolled from supine to prone at age three years, but is not able to crawl, stand or walk, and does not have a pincer grasp. She can bring her hands to the midline and transfer objects from hand to hand. She babbles but does not have any speech, and does not follow commands. She has little interest in her surroundings, and makes occasional eye-contact. She has severe sleep disturbance with reversed sleep-wake cycle, despite treatment with melatonin 4 mg qhs, and obstructive sleep apnea. She also has choreiform movements, hypothyroidism and superficial punctate keratopathy.

On examination at age four years, her height was 72 cm (well below the 3rd centile, 50th centile for 10 months), weight 7.4 kg (well below the 3rd centile, 50th centile for 6 months), and occipito-frontal head circumference (OFC) 43 cm (-4 standard deviations, well below the 3rd centile). She was profoundly hypotonic and brachycephalic with generalized joint laxity. Craniofacial features included bilateral epicanthal folds, bulbous nasal tip, thin vermillion border of the upper lip and low-set ears. (Figure 1A) She was able to make anti-gravity movements of all four limbs but not against resistance. Deep tendon reflexes were 2+ and plantar responses were flexor. Sensation appeared normal. She had occasional choreiform movements but no tremor.

The following investigations were reported as normal: visual evoked potentials, magnetic resonance spectroscopy of the brain, chromosomal microarray (4×180K Cytosure ISCA v2 oligonucleotide platform, Oxford Gene Technology Inc., Oxford, UK), chromosomal breakage studies in blood lymphocytes, plasma amino acids, urine organic acids, plasma lactate, plasma carnitine, plasma thymidine, urinary glycosaminoglycans and oligosaccharides, cerebrospinal fluid analyses (protein, glucose, amino acids, lactate and neurotransmitter metabolites), as well as transferrin iso-electric focusing studies.
An EEG was suggestive of encephalopathy at age 10 months. MRI of the brain revealed global reduction in cerebral volume, a thin corpus callosum, and myelination at the lower limit of normal. Mild non-specific myopathic changes were evident on muscle biopsy.

Subject F2-V.5

This is a 3.9-year-old girl born at 41 weeks after a normal pregnancy. The healthy parents, who are originally from Morocco, are first cousins once removed and she is their fifth child. Family history is otherwise non-contributory. Birth weight was 3158 g and Apgar scores were 8/10/10 after 1/5/10 minutes respectively. Hypotonia was noted from birth but was more prominent at age three months. At age 3.9 years she is a small child with generalized hypotonia. She has been able to sit without support since age 2.5 years but cannot stand. She makes sounds, but has no speech. She has myopathic facies, ptosis, and shallow nasolabial folds. (Figure 1B) Onset of epilepsy with tonic-clonic seizures was at age three years and 10 months. A G-tube was inserted at 3 years for feeding problems and recurrent upper airway infections thought to be related to malnourishment. The following investigations were reported as normal: metabolic screening in urine and blood (age 10 months), chromosomal microarray (Agilent 180K Oligoarray), methylation analysis of the Silver-Russell syndrome critical regions on chromosomes 11 and 7, brain MRI (age 10 months), EEG (age 10 months), opthalmologic exam, visual evoked potentials (age two years and 11 months), brainstem auditory evoked potentials (age 2 years 11 months).

Subject F3-II.1 and Subject F3-II.3

These sisters were born to non-consanguineous healthy parents of Norwegian ethnicity at term with normal birth weights after uncomplicated pregnancies. At ages 15 and 9 years respectively, they remain extremely hypotonic and do not walk without support. Both are normocephalic with OFC in the low normal range. They babble socially, have very communicative body language but no meaningful speech. They are generally content

children but sudden sounds, movements or changes in ambient light frighten them. Tactile aversion, particularly on the soles of the feet, was present in both until about age two years. Chronic constipation has required medical intervention in both. They do not have involuntary movements or stereotypic hand movements and sleep well. They have been treated conservatively for esotropia and the younger girl uses glasses. Vision and hearing appear otherwise normal. On exam, they are short thin girls with dark circles infraorbitally, eyelid ptosis, alternating esotropia, hypotonic facies (Figures 1 C, D) and small hands and feet.

Subject F3-II.1, who was more hypotonic at birth than her sister, was an undemanding baby who slept a lot. She now pulls to a stand from sitting, walks with a walker for up to an hour at a time and uses her hands to bring food to her mouth. Epilepsy was diagnosed at age three years, but in retrospect she most likely had atonic seizures from age six months. Her seizure disorder has been difficult to manage from around age 10 years and a vagal nerve stimulator was implanted at age 12 years. She has only recently had a G-tube placed in order to deliver anti-convulsants more reliably and to supplement oral caloric intake when needed. Her daytime sleepiness seems related to seizure activity and side effects of medications. She has developed a mild scoliosis.

Subject F3-II.3 has been completely G-tube fed since age 11 months. She reacts to nutritional supplements with malaise and vomiting, and therefore receives the majority of her caloric intake as liquefied regular food. She has gastro-oesophageal reflux that

responds to medical treatment. She can manoeuvre from the prone to sitting without assistance and sits stably while using both arms to manipulate toys.

The sisters have experienced multiple seizure types (Table 1), but both display a strikingly similar EEG pattern characterized by encephalopathic background activity with frequent spike and wave discharges (Figure S1).

Cranial MRI was normal in both as were the following investigations: expanded metabolic screening in blood and urine, molecular analysis of *UBE3A, MECP2, MEF2C, FOXG1, CDKL5, TCF4, CNTNAP2, NTNG1, SLC6A8, ZFHX1B/ZEB2, NRXN1, SCN1A, MTHFR* and *DMPK*. Chromosomal microarray with Agilent 105K oligoarray and 250K SNP array showed no disease causing CNVs or regions with absence of heterozygosity.

Supplemental Figures

A

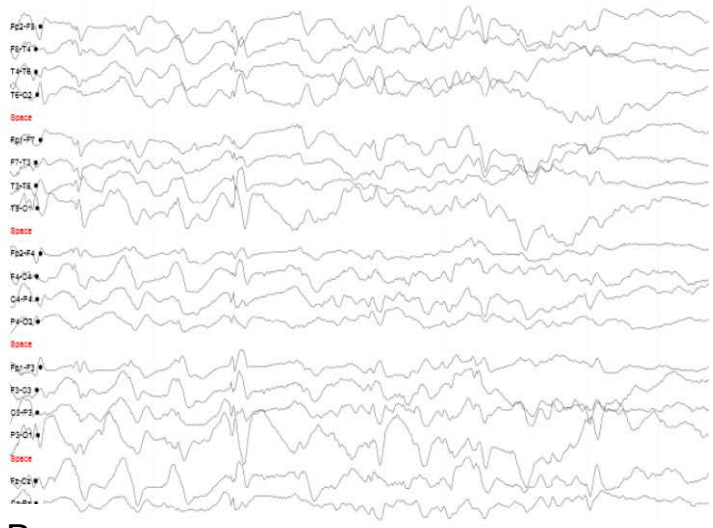

C

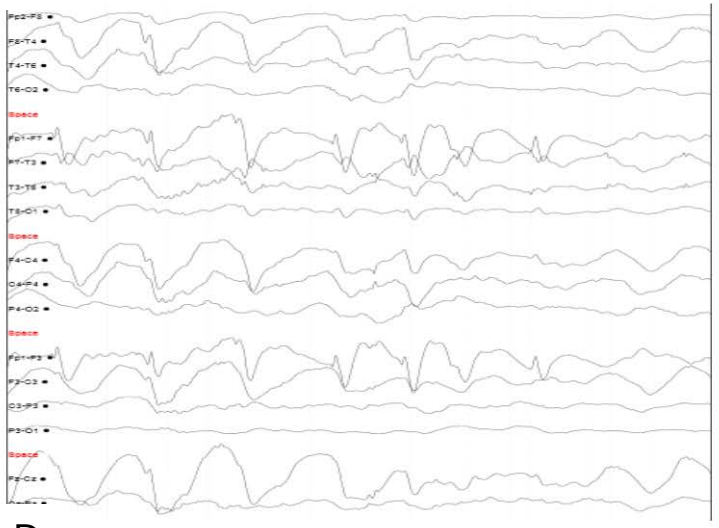

B

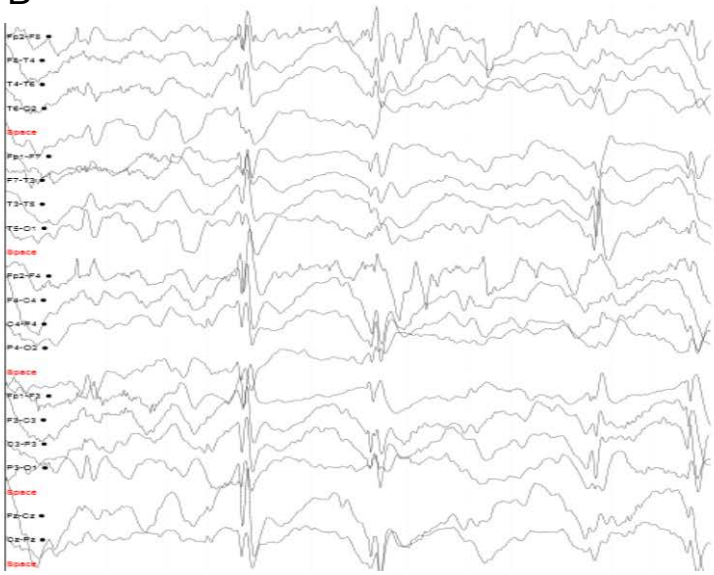

D

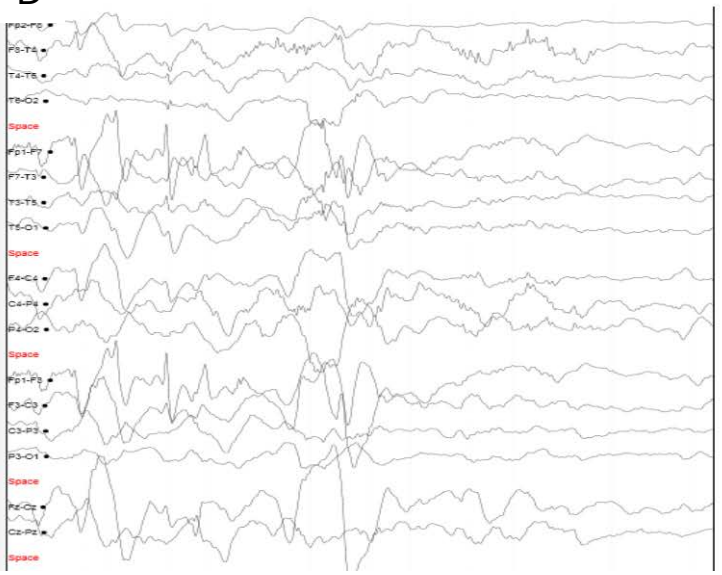

Figure S1. Electroencephalograms (EEGs) from Family 3. EEG of F3-II.1 at 14.5 years of age (**A**) during sleep (**B**) awake. EEG of F3-II.3 at 9 years of age (**C**) during sleep (**D**) awake. The EEGs shows an encephalopathic background with generalized delta-theta activity 3-6 Hz and periodic sharp-slow waves and sharp waves with a fronto-central or multifocal maximum. While sleeping the background activity slowed down to 2-3 Hz with discharges of high amplitude sharp slow waves with a frontal maximum. This EEG pattern observed in the sisters is reminiscent of the pattern seen in individuals with Angelman syndrome. Calibration: longitudinal bipolar montage, 1 second per horizontal unit, 50 μV per vertical unit. Low cut filter 0,53 sec, high cut filter 70Hz, sensitivity 15 μV/mm, Notch on.

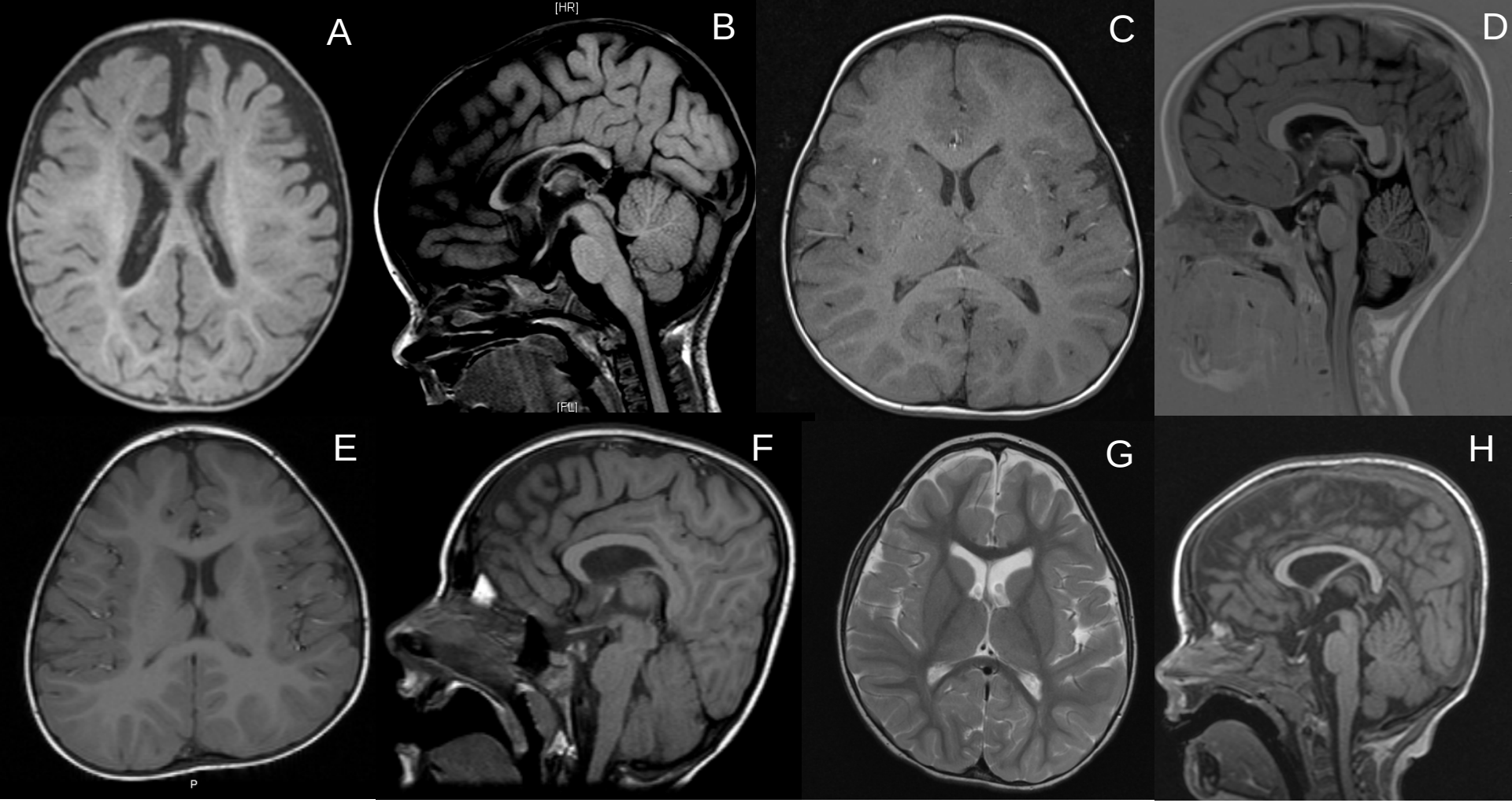
A
B
C
D
E
F
G
H

Figure S2. Neuroimaging results. (A) Axial T1-weighted image and (**B**) sagittal T1-weighted image of Subject F1-IV.1 at 10 months. There is global reduction of cerebral volume and thinning of the corpus callosum. (**C**) Axial T1-weighted image and (**D**) sagittal T1-weighted image of F2-V.5 at 2 years, (**E**) Axial T1-weighted image and (**F**) sagittal T1-weighted image of F3-II.1 at 6 years, (**G**) Axial T1-weighted image and (**H**) sagittal T1-weighted image of F3-II.2 at 2.5 years, demonstrating normal results.

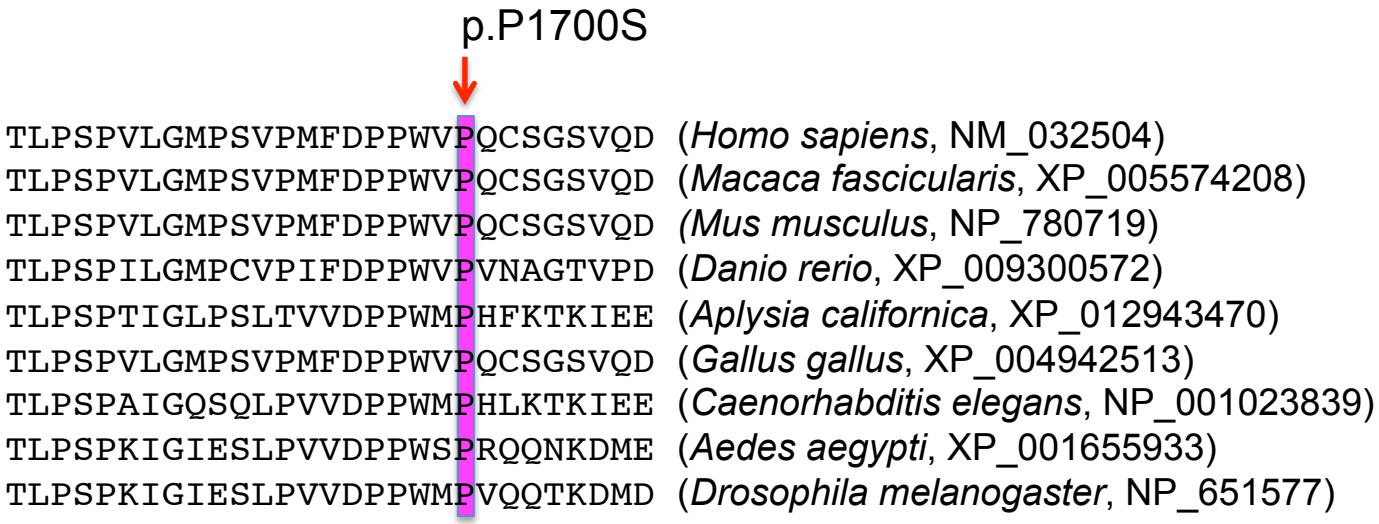
p.P1700S
TLPSPVLGMPSVPMFDPPWVPQCSGSVQD (*Homo sapiens*, NM_032504)
TLPSPVLGMPSVPMFDPPWVPQCSGSVQD (*Macaca fascicularis*, XP_005574208)
TLPSPVLGMPSVPMFDPPWVPQCSGSVQD (*Mus musculus*, NP_780719)
TLPSPILGMPCVPIFDPPWVPVNAGTVPD (*Danio rerio*, XP_009300572)
TLPSPTIGLPSLTVVDPPWMPHFKTKIEE (*Aplysia californica*, XP_012943470)
TLPSPVLGMPSVPMFDPPWVPQCSGSVQD (*Gallus gallus*, XP_004942513)
TLPSPAIGQSQLPVVDPPWMPHLKTKIEE (*Caenorhabditis elegans*, NP_001023839)
TLPSPKIGIESLPVVDPPWSPRQQNKDME (*Aedes aegypti*, XP_001655933)
TLPSPKIGIESLPVVDPPWMPVQQTKDMD (*Drosophila melanogaster*, NP_651577)

Figure S3. Alignment of UNC80 sequences in the Pro1700 region. Species and GenBank accession numbers are in parentheses. Arrow indicates the p.Pro1700Ser variant in Subject F1-IV.1.


NM_032504.1(UNC80):c.7607G>C - [c.7505 (Exon 50) - c.7607+97 (Intron 50)]
Alamut Visual v.2.7 rev. 1
SpliceSiteFinder-like
MaxEntScan
NNSPLICE
GeneSplicer
Human Splicing Finder
5'
3'
Reference Sequence
Mutated Sequence
Branch Points
[0-100]
[0-12]
[0-1]
[0-15]
[0-16]
68.7
7.7
0.7
6.1
75.2
0.0
1.9
79.0
55.4
0.1
64.2
2.2
7580
7590
7607
7607+10
7607+20
7607+30
AACTGCTGGATGTGAAGTCTCACATGAGGTACTGGCCTCGCTTTCCCTGCCCCAAGTGTGAACA
AACTGCTGGATGTGAAGTCTCACATGACGTACTGGCCTCGCTTTCCCTGCCCCAAGTGTGAACA
interactive
biosoftware

Figure S4. Predicted disruption of splicing for the c.7607G>C variant found in Subject F2-V.5. Potential consequences of the c.7607G>C variant on splicing were analyzed using five prediction methods (SpliceSiteFinder-like, MaxEndScan, NNSPLICE, GeneSplicer and Human Splicing Finder; performed with Alamut Visual of Interactive Biosoftware). Ranges of score are indicated in the parentheses right to the methods. Blue and green vertical bars indicate predicted 5' donor and 3' acceptor sites, respectively, with scores indicated for those varying between the wild-type and the variant. Sites with scores unchanged between the wild-type and the variant are dimmed.

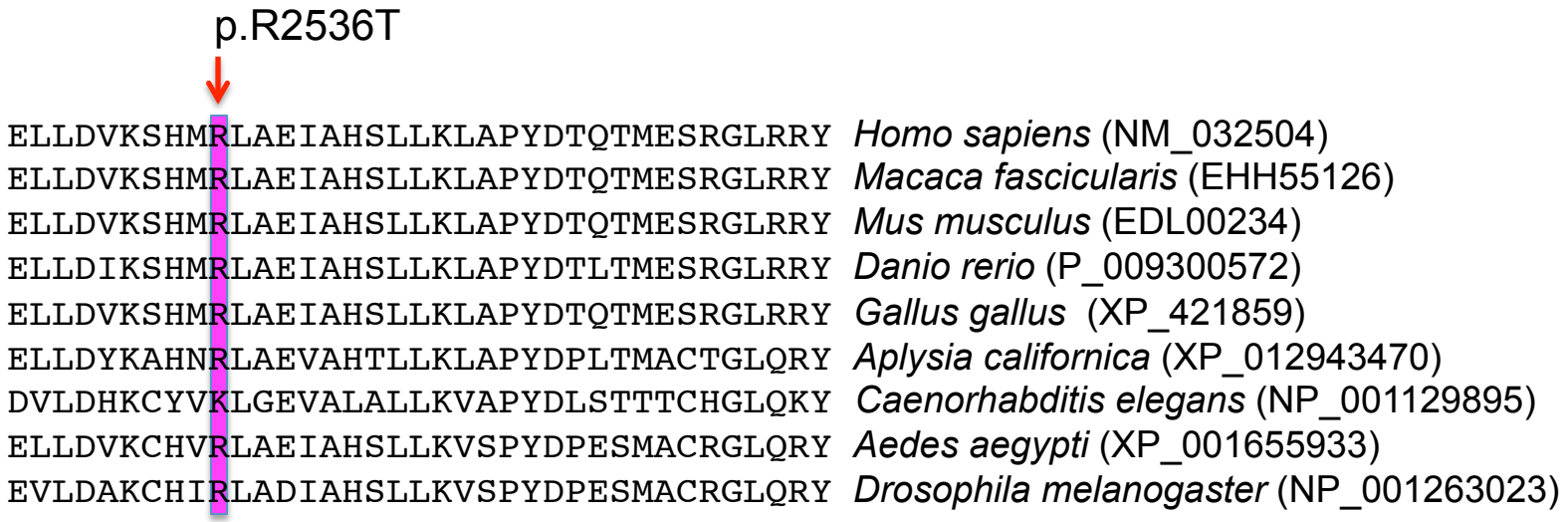
p.R2536T
ELLDVKSHMRLAEIAHSLLKLAPYDTQTMESRGLRRY Homo sapiens (NM_032504)
ELLDVKSHMRLAEIAHSLLKLAPYDTQTMESRGLRRY Macaca fascicularis (EHH55126)
ELLDVKSHMRLAEIAHSLLKLAPYDTQTMESRGLRRY Mus musculus (EDL00234)
ELLDIKSHMRLAEIAHSLLKLAPYDTLTMESRGLRRY Danio rerio (P_009300572)
ELLDVKSHMRLAEIAHSLLKLAPYDTQTMESRGLRRY Gallus gallus (XP_421859)
ELLDYKAHNRLAEVAHTLLKLAPYDPLTMACTGLQRY Aplysia californica (XP_012943470)
DVLDHKCYVKLGEVALALLKVAPYDLSTTTCHGLQKY Caenorhabditis elegans (NP_001129895)
ELLDVKCHVRLAEIAHSLLKVSPYDPESMACRGLQRY Aedes aegypti (XP_001655933)
EVLDAKCHIRLADIAHSLLKVSPYDPESMACRGLQRY Drosophila melanogaster (NP_001263023)

Figure S5. Alignment of UNC80 sequences in the Arg2536 region. Species and GenBank accession numbers are in parentheses. Arrow indicates the p.Arg2536Thr variant in Subject F2-IV.5.

Table S1. Summary of key clinical features in individuals with biallelic mutations in *UNC80* or *NALCN*

	Individuals with *UNC80* mutations				**Individuals with *NALCN* mutations**							
Publication	This report				Köroğlu Ç et al, 2013		Al-Sayed MD et al, 2013					
	Family 1	Family 2	Family 3		Family 5		Family 1			Family 2		
Age (years)	4	4	15	9	20+	20+	7	7	4	17	16	9
Gender	Female	Female	Female	Female	Female	Male	Male	Male	Male	Female	Female	Female
Age at presentation	Birth	Birth	Birth	3 months	Birth	Birth	Birth	Birth	Birth	Birth	Birth	Birth
Persistent hypotonia	+	+	+	+	+	+	+	+	+	-	-	-
Growth history	Failure to thrive, G-tube dependent	Failure to thrive, G-tube dependent	Failure to thrive, supplemental G-tube use	G-tube dependent	Failure to thrive	Failure to thrive	normal	Initial failure to thrive followed by normal growth	Initial failure to thrive followed by normal growth	normal	normal	normal
Severe Intellectual disabilit	+	+	+	+	+	+	+	+	+	+	+	+

y												
Communication	Non-verbal	Non-verbal	Non-verbal	Non-verbal	Non-verbal	Non-verbal	Non-verbal	Non-verbal	Non-verbal	2-word phrases	2-word phrases	2-word phrases
Gross motor function	Non-ambulatory	Non-ambulatory	Walks with support	Walks with support	Non-ambulatory	Non-ambulatory	Non-ambulatory	Non-ambulatory	Non-ambulatory	Walks independently	Walks independently	Walks independently
Seizures	+	+	+	+	+	+	-	-	-	+	+	+
Constipation	+	+	+	+	+	+	+	+	+	+	+	+
Dysmorphic facial features	Hypotonic facies	Hypotonic facies	Hypotonic facies	Hypotonic facies	Prominent forehead, low-set ears, small nose, micrognathia	Prominent forehead, low-set ears, small nose, micrognathia	Triangular facies, prominent nose, smooth philtrum	Triangular facies, prominent nose, smooth philtrum	Triangular facies, prominent nose, smooth philtrum	Triangular facies, prominent nose, smooth philtrum	Triangular facies, prominent nose, smooth philtrum	Triangular facies, prominent nose, smooth philtrum
Brain MRI	Global reduction in cerebral volume, thin corpus callosum	Normal	Normal	Normal	Normal	Cerebellar atrophy	normal	Bilateral parietal white matter abnormalities	Small posterior fossa	normal	normal	normal
Mutation (s)	c.5098 C>T (homozygous)	c.7607 G>C (homozygous)	c.7757T>A/c.2033delA	c.7757T>A/c.2033delA	c.1924 C>T (homozygous)	c.1924 C>T (homozygous)	c.1489delT (homozygous)	c.1489delT (homozygous)	c.1489delT (homozygous)	c.3860 G>T (homozygous)	c.3860 G>T (homozygous)	c.3860 G>T (homozygous)